

A modified Landau–Devonshire thermodynamic potential for strontium titanate

G. Sheng, Y. L. Li, J. X. Zhang, S. Choudhury, Q. X. Jia et al.

Citation: *Appl. Phys. Lett.* **96**, 232902 (2010); doi: 10.1063/1.3442915

View online: <http://dx.doi.org/10.1063/1.3442915>

View Table of Contents: <http://apl.aip.org/resource/1/APPLAB/v96/i23>

Published by the [American Institute of Physics](http://www.aip.org).

Related Articles

Metal induced crystallization mechanism of the metal catalyzed growth of silicon wire-like crystals
Appl. Phys. Lett. **99**, 143102 (2011)

Note: Extraction of hydrogen bond thermodynamic properties of water from dielectric constant and relaxation time data

J. Chem. Phys. **135**, 086101 (2011)

Waste-recycling Monte Carlo with optimal estimates: Application to free energy calculations in alloys

J. Chem. Phys. **135**, 044127 (2011)

Particle-based multiscale coarse graining with density-dependent potentials: Application to molecular crystals (hexahydro-1,3,5-trinitro-s-triazine)

J. Chem. Phys. **135**, 044112 (2011)

Stacking in sediments of colloidal hard spheres

J. Chem. Phys. **135**, 034510 (2011)

Additional information on *Appl. Phys. Lett.*

Journal Homepage: <http://apl.aip.org/>

Journal Information: http://apl.aip.org/about/about_the_journal

Top downloads: http://apl.aip.org/features/most_downloaded

Information for Authors: <http://apl.aip.org/authors>

ADVERTISEMENT

**AIPAdvances**

Submit Now

**Explore AIP's new
open-access journal**

- **Article-level metrics
now available**
- **Join the conversation!
Rate & comment on articles**

A modified Landau–Devonshire thermodynamic potential for strontium titanate

G. Sheng,^{1,a)} Y. L. Li,² J. X. Zhang,^{1,b)} S. Choudhury,¹ Q. X. Jia,³ V. Gopalan,¹ D. G. Schlom,⁴ Z. K. Liu,¹ and L. Q. Chen¹

¹Department of Materials Science and Engineering, The Pennsylvania State University, University Park, Pennsylvania 16802, USA

²Pacific Northwest National Laboratory, Richland, Washington 99352, USA

³Center for Integrated Nanotechnologies, Los Alamos National Laboratory, Los Alamos, New Mexico 87545, USA

⁴Department of Materials Science and Engineering, Cornell University, Ithaca, New York 14853, USA

(Received 22 January 2010; accepted 12 May 2010; published online 7 June 2010)

The range of reported values of the Landau energy coefficients of bulk SrTiO₃ leads to uncertainty in not only the magnitude but also the direction of the calculated spontaneous polarization in SrTiO₃ thin films in a state of biaxial tension. In this study, we use experimental results from strained SrTiO₃ films together with phase-field simulations to refine the values of the Landau energy coefficients and report a modified thermodynamic potential for bulk strontium titanate. The transition temperatures and ferroelectric/antiferrodistortive domain stabilities predicted from this modified potential agree well with measurements on biaxially strained SrTiO₃ thin films. © 2010 American Institute of Physics. [doi:10.1063/1.3442915]

SrTiO₃ has received considerable interest due to its low temperature properties, such as high dielectric constants and low microwave losses, as well as its room temperature applications.¹ Bulk SrTiO₃ is an incipient ferroelectric in its pure unstressed form and undergoes a cubic to tetragonal antiferrodistortive (AFD) transition at 105 K.^{2–5} It has been predicted^{6–10} and experimentally verified^{10–15} that strain can induce room temperature ferroelectricity in SrTiO₃ thin films. Both ferroelectric and AFD domain stabilities in strained SrTiO₃ thin films have been investigated extensively using Landau–Devonshire thermodynamic theory,^{6,7,9,10} where the spontaneous polarization $p=(p_1, p_2, p_3)$ and the structural order parameter $q=(q_1, q_2, q_3)$ are chosen as the order parameters to describe the ferroelectric transition and the AFD transition, respectively. The ferroelectric and AFD domain structures of SrTiO₃ thin films have also been predicted by the phase-field method.^{9,10} In all existing thermodynamic analyses^{6,7,9} and phase-field simulations,^{9,10} a fourth-order polynomial is employed to describe the bulk stress-free free energy density $f_{\text{bulk}}(p_i, q_i)$, as follows:

$$\begin{aligned}
 f_{\text{bulk}}(p_i, q_i) = & \alpha_1(p_1^2 + p_2^2 + p_3^2) + \alpha_{11}(p_1^4 + p_2^4 + p_3^4) \\
 & + \alpha_{12}(p_1^2 p_2^2 + p_2^2 p_3^2 + p_3^2 p_1^2) + \beta_1(q_1^2 + q_2^2 + q_3^2) \\
 & + \beta_{11}(q_1^4 + q_2^4 + q_3^4) + \beta_{12}(q_1^2 q_2^2 + q_2^2 q_3^2 \\
 & + q_3^2 q_1^2) - t_{11}(p_1^2 q_1^2 + p_2^2 q_2^2 + p_3^2 q_3^2) - t_{12}[p_1^2(q_2^2 \\
 & + q_3^2) + p_2^2(q_1^2 + q_3^2) + p_3^2(q_1^2 + q_2^2)] \\
 & - t_{44}(p_1 p_2 q_1 q_2 + p_2 p_3 q_2 q_3 + p_3 p_1 q_3 q_1), \quad (1)
 \end{aligned}$$

where α_{ij} and β_{ij} are the Landau coefficients and t_{ij} is the coupling coefficient between p and q . The range in the Landau energy coefficients leads, however, to significantly different predictions of domain states, and thus different domain structures, under biaxial tensile strain. For example, the

uncertainty of the fourth-order coefficient α_{12} in Eq. (1) will result in two completely different polar states under tensile strains. An α_{12} value of 5.5×10^{-12} cm⁶ dyn/esu⁴ [the average of the experimental value, $\alpha_{12}=9.28$ at $T=8$ K,¹⁶ and the value used in a previous calculation⁷ $\alpha_{12}=1.7$ (both in cgs units 10^{-12} cm⁶ dyn/esu⁴)] favors the ferroelectric polarization along pseudocubic (subscript p) $[010]_p/[100]_p$.⁹ A smaller value, e.g., $\alpha_{12}=1.7$ (Refs. 7 and 9) or 1.5 (Ref. 6) stabilizes a ferroelectric polarization along $[110]_p/[1\bar{1}0]_p$.

To find the appropriate α_{12} value, we compared the simulation results using two existing α_{12} values with available experimental measurements of polarization directions. Optical second harmonic generation measurements demonstrated that a (001) SrTiO₃ thin film grown on (110) DyScO₃ substrate with biaxial strain $e_{s1}=e_{s2}=0.94\%$ (Ref. 12) (e_{s1} stands for the misfit strain between the substrate and thin film along $[100]_p$ while e_{s2} is along the $[010]_p$ axis) exhibited a $[110]_p/[1\bar{1}0]_p$ polar state, which is consistent with both thermodynamic calculations^{6,7} and phase-field simulations⁹ using $\alpha_{12}=1.7$ or 1.5. The $[110]_p/[1\bar{1}0]_p$ polar state, an orthorhombic *Amm*2 structure, also agrees with first-principle calculations.⁸ In contrast, samples with anisotropic in-plane strains, (001) SrTiO₃ on (110) DyScO₃ (Ref. 10) ($e_{s1}=1.03\%$, $e_{s2}=1.06\%$) and (001) SrTiO₃ on (110) GdScO₃ (Ref. 15) ($e_{s1}=1.46\%$, $e_{s2}=1.59\%$) develop ferroelectric polarization along both in-plane $[010]_p$ and $[100]_p$ axes, leading to domain twinning at lower temperatures. To be consistent with these experimental findings $\alpha_{12}=5.5$ should be employed¹⁰ instead of 1.7 or 1.5 in order to produce the $[010]_p/[100]_p$ polar states in these two films.

From these simulations it is obvious that the coefficient α_{12} affects the relative thermodynamic stability of the $[110]_p$ and $[100]_p$ polar states under a biaxial tensile strain. In the early electric field induced Raman scattering measurement,¹⁶ the value of α_{12} is determined from ω_s^\perp , the measured components perpendicular to an applied electric field along the (001)-direction. This phonon frequency ω_s^\perp is the only mea-

^{a)}Electronic mail: shengguang@psu.edu.

^{b)}Current address: Research and Development, Carpenter Technology Corporation, Reading, PA 19601.

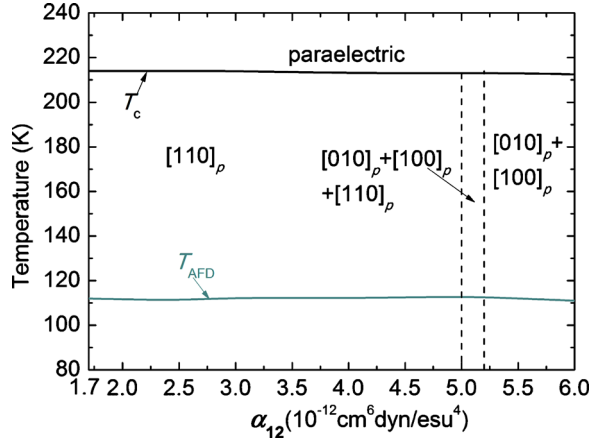


FIG. 1. (Color online) Predicted transition temperatures and polarizations as a function of α_{12} for SrTiO₃ thin films deposited onto (110) DyScO₃ substrates under a symmetric strain of $e_{s1}=e_{s2}=0.94\%$.

sured physical property to determine α_{12} and at the same time, ω_s^\perp is not used to determine other coefficients. Therefore, α_{12} does not affect other physical quantities of SrTiO₃. Thus we are able to adjust α_{12} without changing the other parameters to improve the potential for SrTiO₃.

In this paper, we perform a series of simulations repeating the experimental cooling process in three films with different strain states. In all these simulations we vary α_{12} from 1.7 to 5.5, while fixing all other parameters. After examining the transition temperatures and polarization states as a function of different α_{12} , we identify the most appropriate α_{12} as that satisfying all the existing experimental observations.

In the phase-field model of (001) SrTiO₃ thin films, the temporal and spatial evolutions of the two order parameters p and q are governed by the three-dimensional time dependent Ginzburg–Landau equations, as follows:⁹

$$\frac{\partial p_i(x,t)}{\partial t} = -L_p \frac{\delta F}{\delta p_i(x,t)}, i = 1, 2, 3, \quad (2)$$

$$\frac{\partial q_i(x,t)}{\partial t} = -L_q \frac{\delta F}{\delta q_i(x,t)}, i = 1, 2, 3, \quad (3)$$

where L_p and L_q are the kinetic coefficients. F is the total energy, including the bulk energy, elastic energy, electrostatic energy, and domain wall energy, i.e.,

$$F = \int_V [f_{\text{bulk}} + f_{\text{elas}} + f_{\text{grad}} + f_{\text{elec}}] dV, \quad (4)$$

where $f_{\text{bulk}}(p_i, q_i)$ is same as Eq. (1). The calculation details of other energy terms are addressed in Refs. 9, 17, and 18.

In this work, a (001)-oriented SrTiO₃ thin film on an orthorhombic substrate is considered. The average film/substrate misfit strains $e_{s1}=\bar{\epsilon}_{11}$ and $e_{s2}=\bar{\epsilon}_{22}$ are along the in-plane $[100]_p$ and $[010]_p$ axes, respectively. We took a $128\Delta x \times 128\Delta x \times 40\Delta x$ model size where Δx is the grid spacing. The thickness of the film is $25\Delta x$. The kinetic coefficient in Eq. (1) is taken as $L_q/L_p=180$. The material constants used in the simulation are from the literature^{6,7,9,19} and listed in Ref. 20. These calculations use a background dielectric constant of 10.²¹ Each simulation proceeded for 60 000 time steps (a normalized time step is 0.05).

The transition temperatures and corresponding stable ferroelectric polarization states as a function of α_{12} deter-

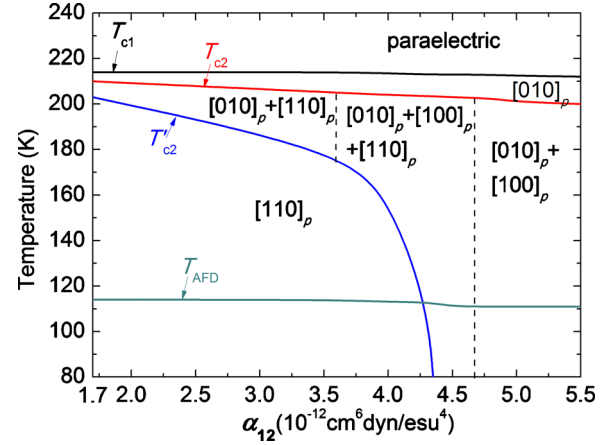


FIG. 2. (Color online) Predicted transition temperatures and polarizations as a function of α_{12} for SrTiO₃ thin film deposited onto (110) DyScO₃ substrates under asymmetric biaxial strains of $e_{s1}=1.03\%$ and $e_{s2}=1.06\%$.

mined from our simulations are summarized in Figs. 1–3 for the three different strains. For symmetric strain $e_{s1}=e_{s2}=0.94\%$ (Fig. 1), there are two transition temperatures on cooling from room temperature: T_c stands for the paraelectric-to-ferroelectric transition temperature and T_{AFD} for the structural transition temperature. The stable ferroelectric polarization directions corresponding to different α_{12} values and temperatures are labeled on the diagram. The stable AFD domains, which appear at temperatures lower than T_{AFD} , are not labeled since they have the same symmetry as earlier formed ferroelectric domains. It can be seen that both T_c and T_{AFD} are nearly independent of α_{12} but the stable direction of the ferroelectric polarization depends strongly on α_{12} . Furthermore the $[110]_p/[1\bar{1}0]_p$ ferroelectric state, the experimentally observed state at symmetric strain, can be obtained by using α_{12} values from 1.7 to as large as 5.0. The $[100]_p/[010]_p$ polar states were predicted with α_{12} values between 5.2 and 6.0, while values between 5.0 and 5.2 resulted in a mixture of the two phases.

For the other two anisotropically strained thin films ($e_{s1}=1.03\%$, $e_{s2}=1.06\%$ in Fig. 2 and $e_{s1}=1.46\%$, $e_{s2}=1.59\%$ in Fig. 3), there are three transition temperatures. The first ferroelectric transition (T_{c1}) corresponds to the development of a polarization along the longer in-plane direc-

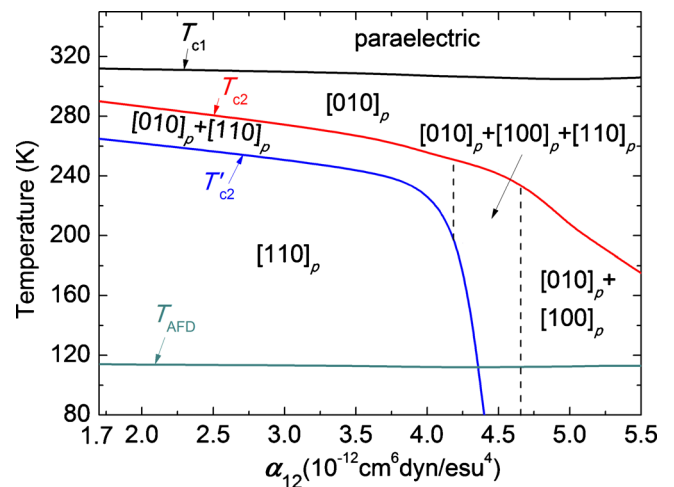


FIG. 3. (Color online) Predicted transition temperatures and polarizations as a function of α_{12} for SrTiO₃ thin film deposited onto (110) GdScO₃ substrates under the asymmetric strains of $e_{s1}=1.46\%$ and $e_{s2}=1.59\%$.

TABLE I. Predicted transition temperatures of SrTiO₃ thin films under the same biaxial strain states utilized in experiments from phase-field simulations using $\alpha_{12}=4.85 \times 10^{-12}$ cm⁶ dyn/esu⁴.

| $e_{s1}=e_{s2}=0.94\%$ | | $e_{s1}=1.03\%, e_{s2}=1.06\%$ | | $e_{s1}=1.46\%, e_{s2}=1.59\%$ | | |
|------------------------|---------------------------|--------------------------------|--------------------------------|--------------------------------|--------------------------------|--------------------------------|
| Experiment | This work | Experiment ^c | This work | Experiment ^d | This work | |
| T_c | ~ 293 K ^a | T_{c1} | ~ 260 K | 215 K | 310 K | |
| | ~ 270 K ^b | | (0, p_2 ,0) | (0, p_2 ,0) | ~ 400 K | |
| T_{AFD} | ($p_1, p_2, 0$) | T_{c2} | ~ 210 K | 210 K | ($p_1, 0, 0$)+(0, $p_2, 0$) | |
| | ~ 180 K ^b | | ($p_1, 0, 0$)+(0, $p_2, 0$) | ($p_1, 0, 0$)+(0, $p_2, 0$) | 210 K | |
| | ($p_1, p_2, 0$) | T_{AFD} | ~ 160 K | 114 K | ~ 150 – 175 K | ($p_1, 0, 0$)+(0, $p_2, 0$) |
| | ($q_1, q_2, 0$) | | ($p_1, 0, 0$)+(0, $p_2, 0$) | ($p_1, 0, 0$)+(0, $p_2, 0$) | ($p_1, 0, 0$)+(0, $p_2, 0$) | ($p_1, 0, 0$)+(0, $p_2, 0$) |
| | | | ($q_2, 0, 0$)+(0, $q_1, 0$) | ($q_2, 0, 0$)+(0, $q_1, 0$) | ($q_2, 0, 0$)+(0, $q_1, 0$) | |

^aReference 12.^bReference 14.^cReference 10.^dReference 15.

tion (i.e., the higher strain axis, here [010]) while the lowest transition temperature (T_{AFD}) corresponds to the AFD transition. The intermediate transition temperature (T_{c2}) produces either twinning from a single variant [010]_p to [010]_p/[100]_p domain structure (with a large α_{12} such as 5.5) or rotation from [010]_p to the [110]_p direction (with smaller α_{12} values such as 1.7). Strictly speaking, the [010]_p to [110]_p transition should be divided into two stages, corresponding to the two intermediate transition temperatures: T_{c2} for the beginning of the transition while T'_{c2} , for the end. As shown in Figs. 2 and 3, an α_{12} value larger than 4.7 is sufficient to stabilize the [010]_p/[100]_p twin structure.

After examining the transition temperatures and polarization states as a function of α_{12} shown in Figs. 1–3, we found that the polarization states predicted from α_{12} values between 4.7 and 5.0 are consistent with all of these recent experiments. An average of 4.85 is then chosen for α_{12} and the transition temperatures determined from this updated α_{12} are summarized in Table I together with experimental measurements. The predicted ferroelectric and AFD domain stabilities are in reasonable agreement with experiments, although the transition temperatures from simulations are always lower than those measured. Such discrepancies, likely, arise from the uncertainties in the electrostriction and thermal expansion coefficients used in the modeling as well as the relaxor character of the films.²²

In summary, we report an improved coefficient α_{12} in the Landau–Devonshire thermodynamic potential for SrTiO₃ utilizing recent experimental data and phase-field simulations. The transition temperatures and ferroelectric/AFD domain stabilities predicted from this modified potential agree well with experimental measurements. It is expected this modified potential will stimulate future experimental measurements of α_{12} and lead to a better understanding of the ferroelectric/AFD domain stabilities in SrTiO₃ thin films.

This work was supported by the DOE under the Grant No. DOE DE-FG02-07ER46417 (Sheng and Chen) and NSF under Grant No. IIP-0737759 (Liu). The computer simulations were carried out on the LION clusters at PSU supported in part by the NSF (Grant Nos. DMR-0820404, DMR-0908718, DMR-9983532, and DMR-0122638) and in part by the Materials Simulation Center and the Graduate Education and Research Services at PSU. The work at LANL

was supported by DOE through the LANL/LDRD Program and the Center for Integrated Nanotechnologies (Jia).

¹R. C. Neville, B. Hoeneisen, and C. A. Mead, *J. Appl. Phys.* **43**, 2124 (1972).²H. Unoki and T. Sakudo, *J. Phys. Soc. Jpn.* **23**, 546 (1967).³P. A. Fleury, J. F. Scott, and J. M. Worlock, *Phys. Rev. Lett.* **21**, 16 (1968).⁴G. Shirane and Y. Yamada, *Phys. Rev.* **177**, 858 (1969).⁵H. Thomas and K. A. Müller, *Phys. Rev. Lett.* **21**, 1256 (1968).⁶N. A. Pertsev, A. K. Tagantsev, and N. Setter, *Phys. Rev. B* **61**, R825 (2000); **65**, 219901(E) (2002).⁷A. K. Tagantsev, E. Courtens, and L. Arzel, *Phys. Rev. B* **64**, 224107 (2001).⁸A. Antons, J. B. Neaton, K. M. Rabe, and D. Vanderbilt, *Phys. Rev. B* **71**, 024102 (2005).⁹Y. L. Li, S. Choudhury, J. H. Haeni, M. D. Biegalski, A. Vasudevarao, A. Sharan, H. Z. Ma, J. Levy, V. Gopalan, S. Trolier-McKinstry, D. G. Schlom, Q. X. Jia, and L. Q. Chen, *Phys. Rev. B* **73**, 184112 (2006).¹⁰M. D. Biegalski, E. Vlahos, G. Sheng, Y. L. Li, M. Bernhagen, P. Reiche, R. Uecker, S. K. Streiffner, L. Q. Chen, V. Gopalan, D. G. Schlom, and S. Trolier-McKinstry, *Phys. Rev. B* **79**, 224117 (2009).¹¹M. P. Warusawithana, C. Cen, C. R. Sleasman, J. C. Woicik, Y. Li, L. F. Kourkoutis, J. A. Klug, H. Li, P. Ryan, L. P. Wang, M. Bedzyk, D. A. Muller, L. Q. Chen, J. Levy, and D. G. Schlom, *Science* **324**, 367 (2009).¹²J. H. Haeni, P. Irvin, W. Chang, R. Uecker, P. Reiche, Y. L. Li, S. Choudhury, W. Tian, M. E. Hawley, B. Craigo, A. K. Tagantsev, X. Q. Pan, S. K. Streiffner, L. Q. Chen, S. W. Kirchoefer, J. Levy, and D. G. Schlom, *Nature (London)* **430**, 758 (2004).¹³R. Wördenweber, E. Hollmann, R. Kutzner, and J. Schubert, *J. Appl. Phys.* **102**, 044119 (2007).¹⁴D. Nuzhnyy, J. Petzelt, S. Kamba, P. Kužel, C. Kadlec, V. Bovtun, M. Kempa, J. Schubert, C. M. Brooks, and D. G. Schlom, *Appl. Phys. Lett.* **95**, 232902 (2009).¹⁵A. Vasudevarao, S. Denev, M. D. Biegalski, Y. L. Li, L. Q. Chen, S. Trolier-McKinstry, D. G. Schlom, and V. Gopalan, *Appl. Phys. Lett.* **92**, 192902 (2008).¹⁶P. A. Fleury and J. M. Worlock, *Phys. Rev.* **174**, 613 (1968).¹⁷Y. L. Li, S. Y. Hu, Z. K. Liu, and L. Q. Chen, *Acta Mater.* **50**, 395 (2002).¹⁸Y. L. Li, S. Y. Hu, and L. Q. Chen, *J. Appl. Phys.* **97**, 034112 (2005).¹⁹H. Uwe and T. Sakudo, *Phys. Rev. B* **13**, 271 (1976).²⁰Materials constants for SrTiO₃ (except α_{12}): $\alpha_1=4.5 \times 10^{-3}[\coth(54/T) - \coth(54/30)]$, $\alpha_{11}=2.1 \times 10^{-12}$, $\beta_1=1.32 \times 10^{26}[\coth(145/T) - \coth(145/105)]$, $\beta_{11}=1.69 \times 10^{43}$, $\beta_{12}=3.88 \times 10^{43}$, $Q_{11}=5.09 \times 10^{-13}$, $Q_{12}=-1.50 \times 10^{-13}$, $Q_{44}=1.065 \times 10^{-13}$, $\Lambda_{11}=8.7 \times 10^{14}$, $\Lambda_{12}=-7.8 \times 10^{14}$, $\Lambda_{44}=-9.2 \times 10^{14}$, $c_{11}=3.36 \times 10^{12}$, $c_{12}=1.07 \times 10^{12}$, $c_{44}=1.27 \times 10^{12}$, $t_{11}=-1.94 \times 10^{15}$, $t_{12}=-0.84 \times 10^{15}$, $t_{44}=6.51 \times 10^{15}$ (in cgs units and T in K).²¹A. K. Tagantsev, *Ferroelectrics* **375**, 19 (2008).²²M. D. Biegalski, Y. Jia, D. G. Schlom, S. Trolier-McKinstry, S. K. Streiffner, V. Sherman, R. Uecker, and P. Reiche, *Appl. Phys. Lett.* **88**, 192907 (2006).